UNIVERSIDADE DE SÃO PAULO

INSTITUTO DE FÍSICA
CAIXA POSTAL 20516
01498 - SÃO PAULO - SP
BRASIL

PUBLICAÇÕES

CORRELATION DIMENSION OF DENSITY FLUCTUATIONS IN TBR-1*

C.P.C. Prado and **N. Fiedler-Ferrari**
Instituto de Física, Universidade de São Paulo

Junho/1990

CORRELATION DIMENSION OF DENSITY FLUCTUATIONS IN TBR-1

C.P.C. Prado and N. Fiedler-Ferrari

Instituto de Física, Universidade de São Paulo

Caixa Postal 20516 - 01498 São Paulo - SP - BRAZIL

ABSTRACT - We report results for the correlation dimension associated with density fluctuations measured by Langmuir probes placed in the scrape-off layer of Tokamak TBR-1. From a judicious use of the Grassberger-Procaccia algorithm we show that there is a low dimension behavior in most of the analyzed signals. We also review the literature and compare our findings with previous results.

1. INTRODUCTION

The theory of dynamical systems has provided new tools to analyze chaotic time signals including the generalized dimensions, the $f(\alpha)$ singularity spectrum, the spectrum of Lyapunov exponents and the Kolmogorov entropy. According to these analyses, the long-time behavior of chaotic nonlinear dissipative dynamical systems can often be associated with an attractor characterized by its fractal or multifractal measures. Given an experimental time series, and assuming the existence of an associated strange attractor, the correlation dimension ν provides an estimate of the complexity of the turbulence. In other words, gives an idea of the minimum number of degrees of freedom necessary to describe the dynamics of the system.

The correlation dimension ν can be computed from an experimental time series using an algorithm developed by Grassberger and Procaccia (1983). In this paper we use the Grassberger-Procaccia algorithm (GPA), with a single time-series reconstruction based on the Takens theorem (Takens, 1980), to analyze density fluctuations measured by Langmuir probes placed in the scrape-off layer of the small size Tokamak TBR-1.

There are several applications of the GPA to Tokamak fluctuating signals. However these signals have been obtained in different machines using different diagnostics. Several physical variables, e.g., magnetic field fluctuations (Arter and Edwards, 1985; Coté et al., 1985; Battiston and Asdex-Team, 1986; Sawley et al., 1986), sawtooth activity (Coté et al., 1985), and density fluctuations (Coté et al., 1985; Sawley et al., 1986; Zweben et al., 1987; Barkley et al., 1988), have been analysed by the GPA. In general, it has not been possible to draw a definitive or unique picture from these results. In particular, recent GPA calculations by Barkley et al. (1988), using TFR data , and a similar analysis by Ströhlein and Piel (1989), in a magnetized plasma column, have shown the importance of an appropriate choice of the sampling frequency to reveal structure within turbulence. In another paper, Zweben et al. (1987), considering TFTR data, employed a local slope analysis to show the non existence of a region of linear scaling. As a consequence, this analysis does not support the possibility of a low dimensional behavior.

In this paper we concentrate on some aspects evoked by the previous publications. From a careful analysis in terms of local slopes, as done by Zweben et al. (1987), we were able to find low dimensional behavior in the TBR-1 data. We have used a small sampling frequency with respect to the coherence time of the signal, but considerably bigger than the frequency used by Barkley et. al. (1988).

This paper is organized as follows. The GPA is shortly summarized in Section 2. In Section 3 we review previous works on the subject. A short description of the experimental conditions and the experimental data from the TBR-1 are given in Section 4. In Section 5 we present our results. Finally , in Section 6 we compare our finds with previous results from the literature.

2. DESCRIPTION OF THE ALGORITHM

The GPA is shortly summarized in the following. Details can be found in the original paper by Grassberger and Procaccia (1983). Given the single time series

$$x_i = x(t_i) \quad , \quad i = 1, 2, ..., N \quad , \tag{1}$$

where the x_i are N regularly spaced measurements in time, we reconstruct (Takens, 1980) a set of m-dimensional vectors

$$\vec{q_i} = (x(t_i), x(t_i + p), ... , x(t_i + (m-1)p)) \quad , \tag{2}$$

where m is the embedding dimension, and p is a fixed time lag which is usually of the order of magnitude of the auto-correlation time, τ_c, associated with the time series. For each value of m we calculate the correlation integral

$$C(L) = \lim_{N \to \infty} 1/N^2 \sum_{\substack{i \neq j = 1}}^{N} \theta(L - |\vec{q_i} - \vec{q_j}|) \quad , \tag{3}$$

where θ is the Heaviside step function, $d_{ij} = |\vec{q_i} - \vec{q_j}|$ is the Euclidean norm of the vector $\vec{q_i} - \vec{q_j}$, and N is the total number of experimental points (N has to be taken sufficiently large to give good statistics).

The correlation integral (3) evaluates the fraction of distances smaller than L. In a plot of log C(L) × log L, for a given value of the embedding dimension m, the data should be on a straight line. The slopes of such lines, for increasing values of m, converge to the correlation dimension ν.

The use of the GPA demands some cautions (Atten and Malraison, 1989). For experimental data, N is obviously finite. As a consequence, for high values of m, when a

large number of points is needed to correctly represent the structure of the attractor, one may lose the linear scaling of log C(L) × log L. Many previous results show that each data set has a different behavior. A judicious analysis of the log C(L) × log L plots has to be made to evaluate if there is indeed a linear scaling region (that is, if the statistics given by the experimental data is good enough), and, if so, up to which embedding dimension such an analysis makes sense. In fact, it is known that we need $m \geq \nu$ or, more strongly, $m \geq 2\nu + 1$ (Takens, 1980; Mañe, 1981; Eckmann and Ruelle, 1985), to guarantee saturation. Thus, if m_f is the final embedding dimension for which no saturation on the slopes of log C(L) × log L is observed, the associated correlation dimension ν, if it exists, is higher than or equal to m_f. Another caution is related with the choice of an appropriate sampling frequency to measure the experimental data. High sampling frequencies may lead to erroneous conclusions, producing spurious correlation dimensions, $\nu \simeq 1$, or introducing an inflexion point in the log C(L) × log L curves. These effects are attributed to the dominance of correlations along the trajectory (Theiler, 1986; Sawley et al., 1987; Ströhlein and Piel, 1989).

3. PREVIOUS RESULTS

As we consider density fluctuations, our emphasis will be on the previous results for this variable. However, we have collected in the Appendix all the available results, to our knowledge, related to applications of the GPA to fluctuations in Tokamaks, in a reversed field pinch (Gee and Taylor, 1985), and to non-linear coupling of ion-sound waves and drift waves in a magnetized plasma column (Ströhlein and Piel, 1989).

Density fluctuations on the TOSCA device (Coté et al., 1985) were measured using CO_2 scattering and double Langmuir probes. The data from CO_2 scattering have not shown any saturation in the slope up to m=7, which seems to indicate a high value for the dimensionality or a noisy behavior. The data from Langmuir probes have shown weak signs

of saturation for the dimensionality, indicating $\nu \simeq 5$ for m=8. No details were given concerning the frequency used to sample the experimental signals.

Density fluctuations were also analyzed on the TCA (Sawley et al., 1986). Fluctuations in the ion saturation current, and floating potential in triple Langmuir probes, as well as TCA line-integrated density fluctuations (obtained using an imaging diagnostic based on the phase contrast method) have been studied. The signals were sampled at a frequency of 2 MHz with a total number of points N=8192. The characteristic time of these fluctuations was found to be about 2–5 μs. A shortest sampling time (sampling frequency of 32 MHz) was also used; in this case the number of available data points was too restrict to yield any finite region of L for which the slope of log C(L) × log L becomes constant. These authors have not found any evidence of saturation in the slope up to m=10.

Floating potential fluctuations in Langmuir probes were analyzed in TFTR (Zweben et al., 1987). Data have been obtained using discharges with neutral beam injection, resulting in broadband turbulent fluctuations in the range 10 – 200 kHz. Except for small regions of linear scaling around one, $\nu \simeq 1$, which were interpreted by Zweben et al. (1987) as simple periodic modes present in the turbulence, no consistent scaling was found at intermediate dimensions. The authors suggested that previous data which show a low dimensionality should be revisited using a more careful analysis in terms of local slopes as they did. No details were given concerning sampling frequencies.

Finally, in TFR (Barkley et al., 1988) there are results for the chord average plasma density fluctuations, obtained using CO_2 laser scattering signals measured at wavenumbers $k_\perp = 6 \, cm^{-1}$ and $k_\perp = 18 \, cm^{-1}$. Two different sampling frequencies (f_s) were employed and three signals analyzed. For $f_s = 100 \, MHz$ they found, in two of the signals, a low correlation exponent whose value, as the authors claim, seems to depend on the wavenumber of the sampled turbulence ($\nu = 2.6 \pm 0.2$ at 6 cm^{-1} and $\nu = 3.2 \pm 0.2$ at 18 cm^{-1}). The third signal was recorded with a sampling frequency $f_s = 5 \, MHz$ and no saturation was observed. In view of these results, and comparing them with those obtained

by Coté et al. (1985) and Sawley et al. (1986), they conclude that, to reveal the structure within turbulence, the sampling time should be sufficiently small with respect to the coherence time of the signal.

If we define the ratio $\tau_R = \tau_c/\tau_s$ we can see that in TFR $\tau_c \simeq 1.5 \, \mu s$ and low dimensionality was obtained with $\tau_s = 0.01 \, \mu s$, that is, with a time ratio $\tau_R = 150$; when a sampling time $\tau_s = 0.2 \, \mu s$ was used, with a corresponding $\tau_R = 7.5$, no saturation in the slope was observed. In TCA (Sawley et al., 1986) $\tau_c = 2 - 5 \, \mu s$ and $\tau_s = 0.5 \, \mu s$, giving $\tau_R = 4-10$; for this time ratio, also no evidence of low dimensionality was found. In the same device, for $\tau_c = 0.03 \, \mu s$, that is $\tau_R = 67 - 167$, no region of linear scaling was found.

4. EXPERIMENTAL DATA

TBR-1 is a small circular cross-section Tokamak with a minor radius a = 0.11 m and a major radius R = 0.30 m, operating with ohmically heated plasmas with the following typical parameters: toroidal magnetic field B = (4 – 4.5) kG; plasma current (4 – 10) kA, electron density $(2 - 10)E + 12 \, cm^{-3}$ and electron temperature on axis Te(0) = 100 eV.

The data analyzed in this paper (de Sá et al., 1987) consist of local fluctuating signals of the ion saturation current in triple Langmuir probes placed in the scrape-off layer of TBR-1. The measured signals are proportional to the density broadband fluctuations in the edge of the plasma. The associated frequency spectra are wide, covering the range 10 kHz – 500 kHz. For frequencies f < 100 kHz they are flat in average. Beyond 100 kHz the amplitudes are decaying functions of the frequency with a power law behavior $f^{-\alpha}$ with $\alpha = 2.0 - 3.5$.

The set of four signals we analyze (Fig. 1) represent typical data chosen among the available experimental results. The total number of data points ranges from 11,600 to 15,000. We have a total sampling time varying from 2.90 ms to 3.75 ms while the plasma current is nearly constant. The auto-correlation times associated with the signals range

from 0.5 μs to 6.4 μs. In Table I we specify, for each signal, the values of the relevant parameters.

Fig. 1 around here

Table I around here

The signals have all been sampled at frequency f_s = 4 MHz, with a sampling time τ_s = 0.25 μs and a time ratio τ_R varying between 2 and 26. These values correspond to twice the sampling time employed in TCA by Sawley et al. (1986) and not very different in comparison with one of the sampling times used by Barkley et al. (1988) which did not show low dimensionality.

5.RESULTS OF THE ANALYSIS

As already mentioned, we have applied the GPA to four representative time series. The m-dimensional vectors (Eq. 2) were reconstructed with a time lag comparable to the auto-correlation time, τ_c, which means a time step of 20 sampling intervals in signals JA1001, DZ1045 and JA1052, and of 2 sampling intervals in signal DZ1049 which has a much shorter τ_c (see Table I). The sensitivity of the final results to the choice of the time step was almost none. We obtained essentially the same results for time steps varying from 5 to 50 (JA1001, DZ1045 and JA1052) and from 2 to 20 (DZ1049). Table II illustrates this fact. We present results for two different choices of the time step for signal DZ1049. The differences are all within the computed error and, what is most important , the qualitative behavior (no convergence up to m = 10 in this case) is the same. Similar results were

obtained for all other analyzed signals. A step choice far from τ_c seemed only to reduce the linear scaling region in the log C(L) × log L curves.

Table II around here

The computer program, which had already been tested (Prado and Fiedler-Ferrari, 1989) takes advantage of the floating-point representation of numbers used in some computers. The drastic reduction in CPU time has allowed the classification of all $M(M-1)/2$ distances between the M reconstructed vectors for each embedding dimension m. We have preferred to adopt this last procedure as there seems to be some doubts about the efficiency of the simplified procedure (Malraison et al., 1983 and Atten et al., 1986) used in many previous works. This simplified procedure consists in the computation of the distances between the M reconstructed vectors and a randomly chosen set of a few reference vectors. This procedure also decreases processing time but seems to reduce the useful range where we find a linear scaling in the log C(L) × log L curves (Parker and Chua, 1987).

The program was run in a VAX-11/780 and the resulting curves of $\log_2 C(L) \times \log_2 L/L_0$ (L_0 being an arbitrary constant) are plotted in Fig. 2. Lack of statistics affected curves for dimensions higher than eight, except for signal DZ1049 for which we were able to compute the correlation integral up to embedding dimension 10, and signal JA1052 for which this effect was observed only for m higher than 9. This lack of statistics produces a blurring or drastically reduces the region of linear scaling.

Fig. 2 around here

The linear scaling region was localized by a local slope analysis. The slope of a straight line of every three points of $\log_2 C(L) \times \log_2 L/L_0$ curves was calculated and plotted as a function of the middle point (see Fig.3). From the pictures it is clear the existence of three different regions. Region I, corresponding to the smallest values of L,

and located to the left of the first vertical dashed line in Figs. 2 and 3, is contaminated by lack of statistics. Region III, corresponding to the largest values of L and located to the right of the second dashed line, shows a constant decrease in the value of the slope, due to the fact that the hyper spheres associated with these large values of L cover almost all the attractor. In region II, between the vertical dashed lines, we can see that the slope oscillates about an average constant value. These oscillations may be either intrinsic (Smith, 1988; Ramsey and Yuan, 1989), caused by the lacunarity of the attractor, or caused by the limited amount of data. We consider region II and fit a straight line taking into account all the points in this region for each embedding dimension m. For sure there is some arbitrariness in the choice of the data points belonging to region II. If we consider one extra point, or remove one point, in one of the extremities of the chosen region the value of the slope will change a bit, usually more than the error given by the linear regression methods. We used this information to evaluate what we have considered a realistic error bar to our results, as described in the next paragraph.

Fig. 3 around here

In order to evaluate the error we calculate the slope of points in region II, as well as the slope of points in four or five other slightly different regions obtained by the inclusion or the exclusion of one or two points in the extremities. The final result was the average value between the smallest and the biggest slope. Half of the difference between these values has been adopted as the error. A typical result of this procedure is presented in Table III. As can be seen, the variations in slope due to a particular choice of the linear regression region are almost within the linear regression standard errors. Hence, the final results are not significantly affected by this choice. However, the final errors are about twice the errors obtained previously and are more realistic once they include the uncertainness in finding exactly which data points do belong to the linear scaling range.

Table III around here

Final values for ν were obtained as an average of slope values of embedding dimensions ranging from 5 to 8 for signal JA1001, 5 to 7 for signal DZ1045, and 6 to 9 for signal JA1052. Final results are plotted in Fig. 4 and show an obviously different behavior between signals JA1001, DZ1045, and JA1052, for which the slopes converged to $\nu = 3.3 \pm 0.1$, $\nu = 3.3 \pm 0.1$, and $\nu = 4.4 \pm 0.2$, respectively, and signal DZ1049, for which there was no convergence up to embedding dimension 10 (which means $\nu \geq 10$). These results are also presented in Table IV. This Table includes results obtained for embedding dimensions 9 and 10 (convergent signals) and 11, 12 and 15 (non convergent signals), although they were not considered to estimate the final value of ν, except for m = 9 in signal JA1052.

Fig. 4 around here

Table IV around here

For all signals in the convergent group the error increases and the slope decreases for m = 9 and 10. However, from a careful analysis of the curves of the local slope versus $\log_2 L/L_0$ for these embedding dimensions, it is clear there is no linear scaling. Linear scaling was already not good for m = 8 in signal DZ1045 and was good up to m = 9 in JA1052.

For signal DZ1049 we have obtained good linear scaling up to m = 10. For higher embedding dimensions the linear scaling region did not disappear, as in the previous case, but has been strongly reduced. The values presented in Table IV for m = 11, 12 and 15 refereed to the slopes of these narrower intervals and suggest a non convergent behavior up to embedding dimension 15. For those higher embedding dimensions, if we consider the

whole range of L we see that the slopes stop growing and simulate a false convergence. This emphasizes the importance of a judicious choice of the linear scaling range in the $\log C(L) \times \log L$ curves.

6. DISCUSSION AND CONCLUSIONS

The Grassberger-Procaccia algorithm was applied to density broadband fluctuation signals measured by Langmuir probes placed in the scrape-off layer of the Tokamak TBR-1.

Experimental signals were recorded using a 4 MHz acquisition system. Four representative signals have been analyzed. Three signals showed a low dimensional behavior. Two of them with the same correlation dimension, $\nu = 3.3 \pm 0.1$, and another with a somewhat higher dimensionality $\nu = 4.4 \pm 0.2$. For a fourth signal, which has the shortest auto-correlation time, the slopes did not converge up to embedding dimension $m = 10$, indicating either a higher dimensionality, $\nu \geq 10$, or a noisy behavior.

A careful analysis in terms of local slopes has allowed the identification of domains of the parameter L where the $\log_2 C(L) \times \log_2 L/L_0$ curves display a linear scaling. We are thus able to unambiguously calculate the slopes, unlike in the case of the TFTR results (Zweben et al., 1987) where this linear scaling was not found.

Although our results are not inconsistent with those obtained in TFR (Barkley et al., 1988), especially with respect to the influence of the sampling frequencies used to record the experimental data, some remarks should be made. Let us compare the values of the time ratio between the auto-correlation time and the sampling time, τ_R, in the cases of TFR and TBR-1. In TFR no saturation was observed for $\tau_R = 7.5$ (which is consistent with $\tau_R = 4 - 10$ in TCA for which no saturation was observed) and low dimensionality was found for $\tau_R = 150$ (although no linear scaling has been found in TCA for $\tau_R = 67-167$). Our results show low dimensionality for $\tau_R = 20 - 26$ and no saturation for $\tau_R = 2$.

Our results generally agree with those obtained in TFR. In fact, the sampling time should be sufficiently small with respect to the coherence time of the signal ($\tau_R >> 1$). We did not observe saturation of the derivative in signal DZ1049, which has a small time ratio, $\tau_R = 2$. However, our results, which show low dimensionality, indicate that saturation can be observed with time ratios considerably smaller than those used in TFR ($\tau_R = 150$ in TFR, $\tau_R = 20$–26 in TBR-1). As a final remark, it should be stressed that this sort of reasoning involving sampling frequencies does not exclude the possibility that a particular signal has a noisy behavior even if recorded with a high frequency acquisition system.

Results for the correlation dimension of density fluctuations in TBR-1 Tokamak presented in this paper, together with those obtained in TOSCA and TFR devices, reinforce the idea that low dimensionality can be found in these signals indicating the possibility of a small number of fundamental processes governing the turbulence. On the other hand, some signals continue to show a higher dimensionality. Additional efforts should be done in order to answer some questions: (a) Are these higher dimensionalities intrinsic to the signals, indicating a noisy behavior?; (b) Are they consequences of external factors as sampling frequencies, electronic noise added to the experimental data or filtering process?; (c) If external factors are unimportant and high dimensionalities are intrinsic, why some signals are "simpler" than others? Concerning this last question we believe that this picture, with a changing behavior depending on the signal, is consistent with the fact that different signals, associated with the same physical variable, may actually have different histories involving more or less complex processes. These results either in low dimensionality with a picture of turbulence related to a small number of degrees of freedom, or in high dimensionality manifested in the non-saturation at low embedding dimensions.

REFERENCES

Arter W. and Edwards D.N. (1985) 12th Europ. Conf. Contr. Fus. and Plasma Physics, vol. 2, 442.

Atten P., Caputo J.G., Malraison B. and Gagne Y. (1986), Dimensions and Entropies for Chaotic Systems (edited by Mayer-Kress), Springer, p. 180.

Atten P. and Malraison B. (1989) "Le Chaos - Théorie et Experiences", P. Bergé (ed.), Eyrolles, p. 283.

Barkley H.J., Andreoletti J., Gervais F., Olivain J., Quemeneur A. and Truc A. (1988) Plasma Phys. Contr. Fusion 30, 217.

Battiston L. and ASDEX-Team (1986) 13th Europ. Conf. Contr. Fus. and Plasma Physics, vol. 2, 81.

Coté A., Haynes P., Howling A., Morris A.W. and Robinson D.C. (1985) 12th Europ. Conf. Contr. Fus. and Plasma Physics, vol. 2, 450.

de Sá W.P. (1987) Master's Dissertation, University of São Paulo; da Cruz D.F. (1987) Master's Dissertation, University of São Paulo; de Sá W.P., da Cruz D.F. and Galvão R.M.O., to be published.

Eckmann J.P. and Ruelle D. (1985) Rev. Mod. Phys. 57, 617.

Gee S.J. and Taylor J.B. (1985) 12th Europ. Conf. Contr. Fus. and Plasma Physics, vol. 2, 446.

Grassberger P. and Procaccia I. (1983) Phys. Rev. Lett. 50, 346; and Physica 9D, 189.

Malraison B., Atten P., Berge P. and Dubois M. (1983) J. Physique Lett. 44, 897.

Mañé R. (1981) Lecture Notes in Mathematics 898, 230.

Parker T.S. and Chua L.O. (1987) Proc. IEEE, vol. 75, 982.

Prado C.P.C. and Fiedler-Ferrari N. (1989) Phys. Lett. A135, 175.

Ramsey J.B. and Yuan H.J. (1989) Phys. Lett. 134, 287.

Sawley M.L., Simm W., Skiff F. and Pochelon A. (1986) Helvetica Physica Acta 59, 1070; Simm C.W., Sawley M.L., Shiff F. and Pochelon A. (1987) Helvetica Physica Acta 60, 510.

Smith L.A. (1988) Phys. Lett. A133, 283.

Ströhlein G. and Piel A. (1989) Phys. Fluids B1 (6), 1168.

Takens F. (1980) in: Proc. Warwick Symp. 1980, D. Rand and B.S. Young, eds.; Lectures Notes in Math. 898 (Springer, Berlin, 1980), p. 366.

Theiler J. (1986) Phys. Rev. A34, 3427.

Zweben S.J., Manos D., Budny R.V., Efthimion P., Fredrickson E., Greenside H., Hill K.W., Hiroe S., Kilpatrick S., McGuire K., Medley S.S., Park H.K., Ramsey A.T. and Wilgen J. (1987) Journal of Nuclear Mat. 145-147, 250.

FIGURE CAPTIONS

Fig. 1.
Set of four signals analyzed in this paper. Each signal is proportional to density broadband fluctuations in the edge of TBR-1 Tokamak. The amplitude of the signals is represented in arbitrary units (the same for the four signals). In order to show in detail the fluctuations, we plotted data for a short time interval corresponding to 200 μs (the total sampling times are indicated in Table I).

Fig. 2.
Curves of $\log_2 C(L) \times \log_2 L/L_0$ for each analyzed signal and several embedding dimensions m. The domains of the parameter L between the two vertical dashed lines correspond to the linear scaling regions localized by a local slope analysis (Fig. 3).

Fig. 3.
Local slope analysis of the signals. The slope of a straight line of every three points of the $\log_2 C(L) \times \log_2 L/L_0$ curve was calculated and plotted as a function of the middle point. Between the two vertical dashed lines the local slope oscillates about an average value, defining in this way a region of linear scaling. It is evident, comparing the four plots, the different behavior (non-saturation) of the local slope in the linear scaling region of signal DZ1049.

Fig. 4.
Slope values of $\log_2 C(L) \times \log_2 L/L_0$ as a function of the embedding dimension. Signals JA1001, JA1052 and DZ1045 show a clear saturation of the slope as m increases. Values for ν were obtained as an average of saturated values of the slope. The two horizontal solid lines give, respectively, the lower and upper bound for the ν value. For signal DZ1049 there was no convergence up to m = 10, which means $\nu \geq 10$.

APPENDIX

CORRELATION DIMENSION FOR FLUCTUATING SIGNALS IN PLASMAS FOR FUSION

MACHINE	SIGNAL	DIAGNOSTIC	CORRELATION DIMENSION	PARTICULARITY
DITE (Arter and Edwards, 1985)	$\dot{B}_\theta$	Mirnov Coils	$\nu = 2.1 \pm 0.3$	Ohmic, non-diverted discharge, $f_s = 40$ kHz
TOSCA (Coté et al., 1985)	$\dot{B}_r$	Mirnov Coils	$\nu = 2.4 \pm 0.1$	Coherent m=2, n=1 mode ($\delta B/B < 10^{-3}$)
	$\bar{n}_e$ (chord average), m=2 activity	CO_2 laser scattering	No saturation ($\nu > 7$)	
	Saturation current i_s	Langmuir probes	Weak signs of saturation ($\nu=5$ when m=8)	
JET (Coté et al., 1985)	MHD activity	Mirnov Coils	No saturation	No coherent mode activity, but only low level turbulent fluctuation ($\delta B/B \approx 10^{-6}$)
			$\nu = 2.4 - 2.9$	Coherent mode activity with primarily m=2, n=1 or m=3, n=1
			$\nu \approx 3$	Current rise phase
			$\nu = 2.4$	Oscillating m=2, n=1 activity associated with the precursor to disruption (also 25% of n=2 present)
			$\nu \approx 4$	Post disruption (magnetic activity large and highly turbulent) and locked mode phase prior to disruption (irregular activity with small mini-disruption)
	Sawtooth activity	Soft X-Ray diodes ECE diagnostic	$\nu \approx 1$	
HBTX1A Reversed field pinch (Gee and Taylor, 1985)	$\dot{B}_\phi$, $\dot{B}_\theta$	Mirnov coils Si surface barrier diodes	$\nu = 5 - 7$	

(to be continued)

Experiment	MHD activity / measured quantity	Diagnostic	ν	Comments
ASDEX Different phases of a typical high power NI-heated discharge (Battiston and Asdex Team, 1986)	MHD activity	Mirnov coils	$3 < \nu < 3.75$	Probe coil externally in the equatorial plane
		Soft X-rays signals	$\nu \approx 1$	Edge soft X-rays signals, all phases (q>1)
			$1 < \nu < 3.5$	Central soft X-rays signals passing from L to H phase (q<1). $f_s = 2$ MHz, $\tau_c = 2 - 5\ \mu s$
TCA (Sawley, 1986)	$\dot{B}_\theta$	Mirnov coils	No saturation ($\nu \geq 10$)	Discharges with neutral beam injection
	Saturation current $\tilde{I}_s$	Langmuir probes		
	Floating potential $\tilde{V}_f$	Langmuir probes		
	Line integrated density fluctuation	Image diagnostic based on the phase contrast method		
TFTR (Zweben et al., 1987)	Floating potential $\tilde{V}_f$	Langmuir probes	No saturation (no linear scaling found in the log (L) x log L plot)	
TFR (Barkley, 1988)	Chord average density fluctuation	CO_2 laser scattering	$\nu = 2.6 \pm 0.2$ and $\nu = 3.2 \pm 0.2$	$f_s = 100$ MHz, $\tau_c \approx 1.5\ \mu s$
			No saturation	$f_s = 5$ MHz, $\tau_c \approx 1.5\ \mu s$
Magnetized plasma column (Ströhlein and Piel, 1989)	Saturation current $\tilde{I}_s$	Langmuir probes	$\nu = 3.9 \pm 0.2$ and $\nu = 4.8 \pm 0.2$	Non-linear coupling of ion-sound waves and drift waves, $f_s = 200$ kHz. Coherent case
			No saturation ($\nu \geq 7$)	Non coherent (broad band fluctuations)

f_s = sampling frequency ; τ_c = auto-correlation time

Signal	N	Total sampling time (ms)	τ_c (μs)	τ_R
JA1001	12,000	3.00	4.9	20
DZ1045	15,000	3.75	5.3	21
JA1052	11,600	2.90	6.4	26
DZ1049	12,000	3.00	0.5	2

Table I - Number of data points, N, total sampling time, auto-correlation time, τ_c, and time ratio, $\tau_R = \tau_c/\tau_s$, for each one of the analyzed signals. The signals were sampled at frequency $f_s = 4$ MHz ($\tau_s = 0.25\ \mu s$).

Embedding Dimension	2	3	4	5	6	7	8	9	10
time step 2	1.89±0.20	2.73±0.18	3.56±0.13	4.40±0.17	5.28±0.21	6.17±0.24	7.00±0.23	7.85±0.32	8.61±0.27
time step 20	1.79±0.23	2.66±0.16	3.55±0.10	4.47±0.13	5.44±0.16	6.41±0.19	7.37±0.22	8.26±0.26	8.83±0.35

Table II - Slopes of $\log C(L) \times \log L$ for two different choices of the time step for signal DZ1049. The auto-correlation time corresponds to step 2.

m \ Range	1	2	3	4	5	Final Result
2	1.71±0.06	1.70±0.05	1.63±0.04	1.69±0.05	1.75±0.06	1.70±0.11
3	2.36±0.05	2.34±0.05	2.28±0.03	2.33±0.05	2.40±0.06	2.36±0.11
4	2.86±0.04	2.86±0.03	2.81±0.04	2.83±0.04	2.89±0.04	2.85±0.08
5	3.27±0.03	3.27±0.03	3.25±0.04	3.25±0.03	3.29±0.04	3.27±0.06
6	3.43±0.03	3.41±0.03	3.43±0.04	3.44±0.03	3.42±0.03	3.43±0.05
7	3.40±0.04	3.37±0.04	3.40±0.05	3.44±0.04	3.37±0.04	3.41±0.08
8	3.24±0.06	3.21±0.05	3.25±0.06	3.30±0.06	3.19±0.05	3.25±0.11
9	3.02±0.06	3.01±0.06	3.03±0.08	3.10±0.07	2.96±0.06	3.04±0.14
10	2.86±0.06	2.87±0.05	2.83±0.07	2.93±0.07	2.81±0.06	2.88±0.13

Table III - Typical oscillations in the values of the slope due to the particular choices of the linear regression region. Different ranges correspond to a basic region in L. Slightly different regions are obtained by inclusion or exclusion of one or two points in the extremities. The final slope is the average value between the smallest and the biggest slopes. Results are for signal JA1001.

Embedding Dimension	Slope			
	JA1001	DZ1045	JA1052	DZ1049
2	1.70±0.11	1.84±0.08	1.59±0.09	1.89±0.20
3	2.36±0.11	2.58±0.08	2.40±0.14	2.73±0.18
4	2.85±0.08	3.07±0.05	3.17±0.14	3.56±0.13
5	3.27±0.06 *	3.34±0.03 *	3.83±0.13	4.40±0.17
6	3.43±0.05 *	3.36±0.10 *	4.34±0.08 *	5.28±0.21
7	3.41±0.08 *	3.20±0.13 *	4.52±0.05 *	6.17±0.24
8	3.25±0.11 *	3.05±0.10	4.49±0.17 *	7.00±0.23
9	3.04±0.14	2.93±0.08	4.25±0.25 *	7.85±0.32
10	2.88±0.13	2.82±0.11	3.94±0.26	8.61±0.27
11	–	–	–	9.19±0.37
12	–	–	–	9.67±0.23
15	–	–	–	10.62±0.41

Table IV - Final slope values for each analyzed signal. Values marked with an asterisk
were used to compute the correlation dimension. Results for signal DZ1049
for embedding dimensions m = 11, 12 and 15 were obtained in narrower
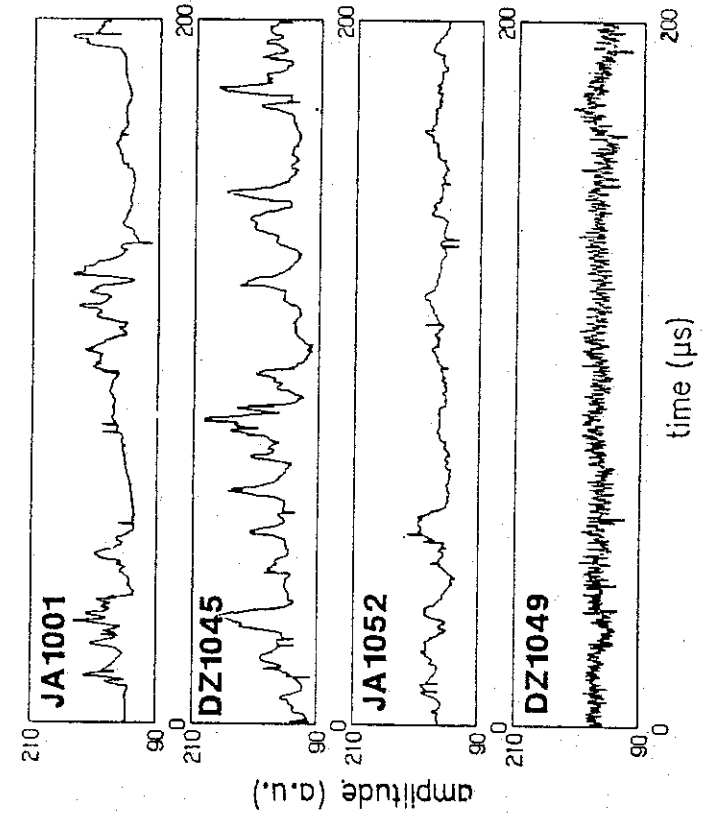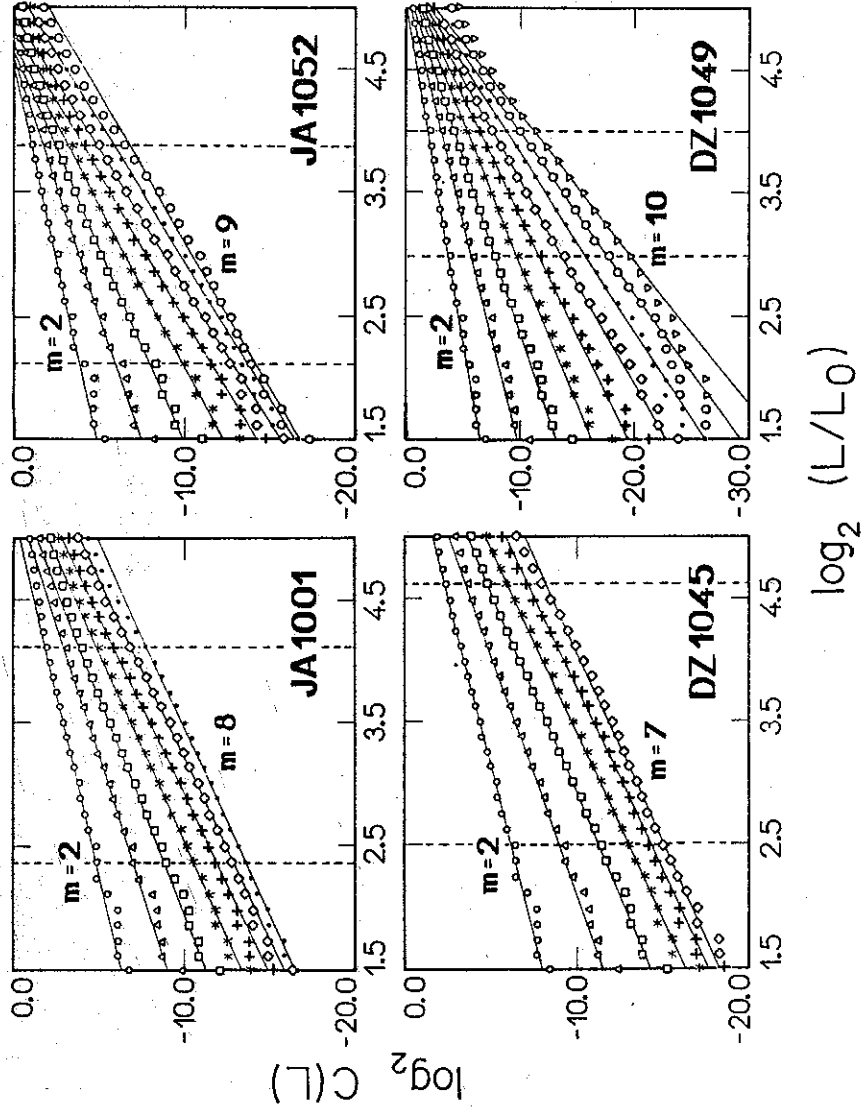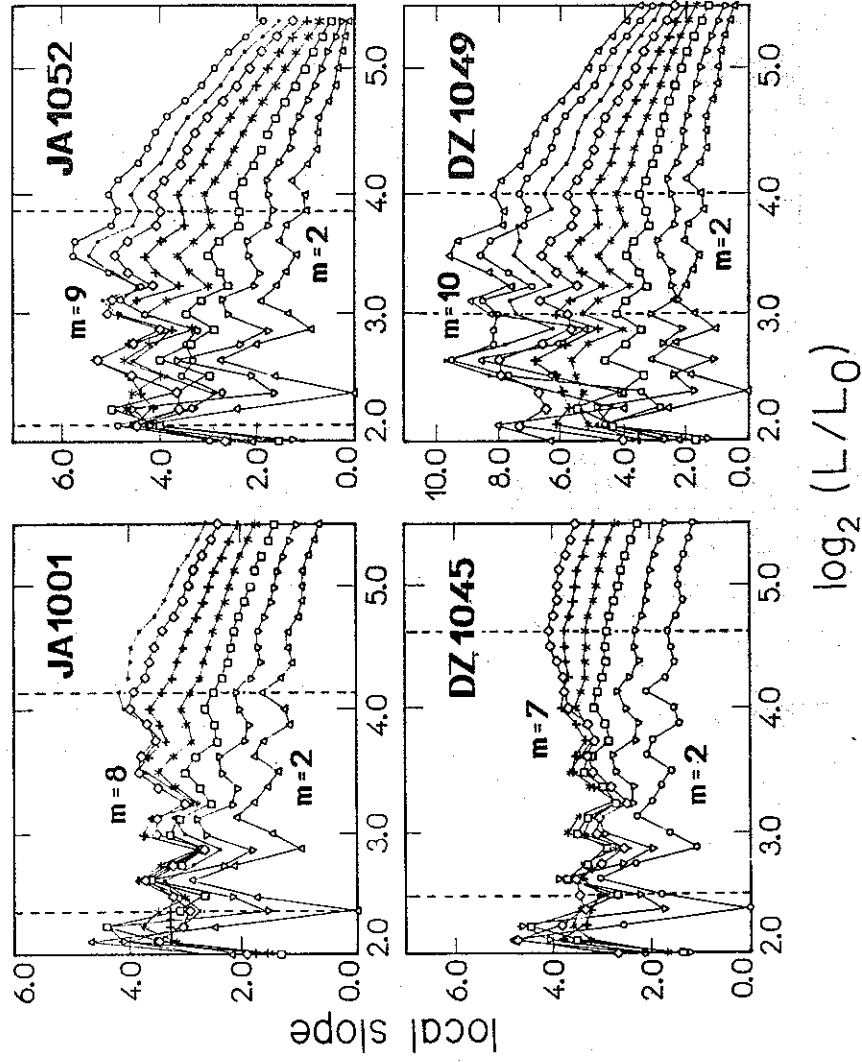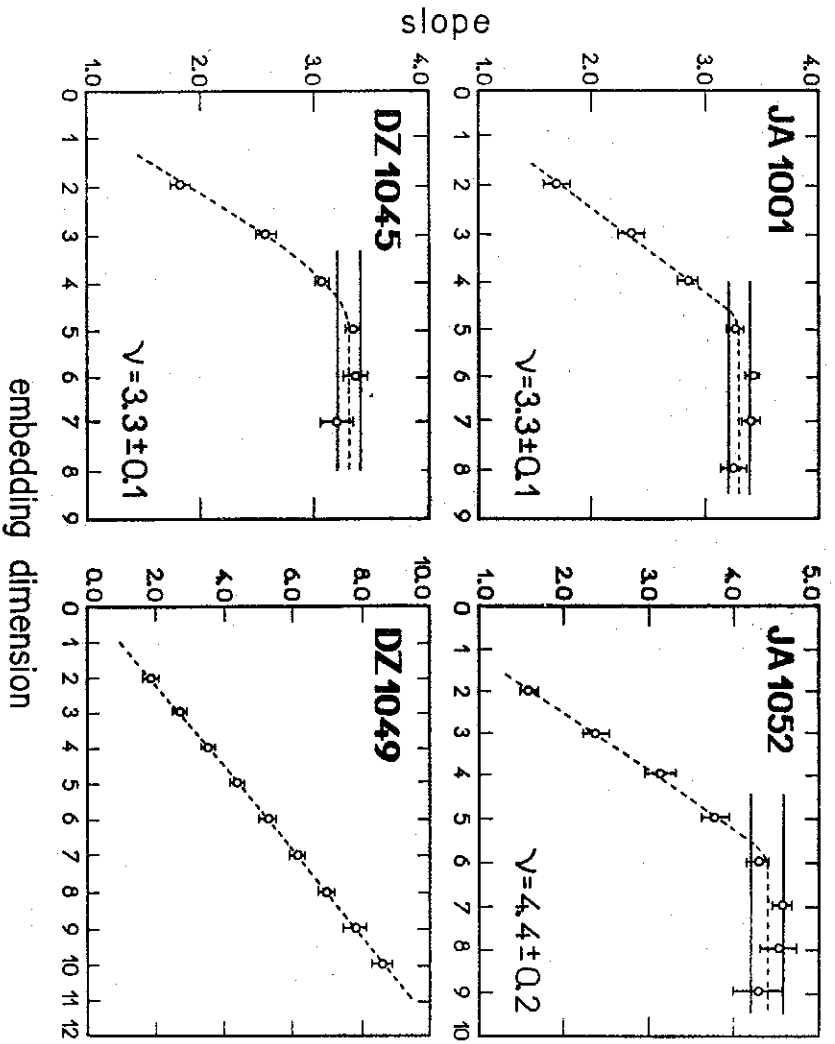regions of linear scaling.

Fig.1

Fig. 2

Fig. 3

Fig. 4